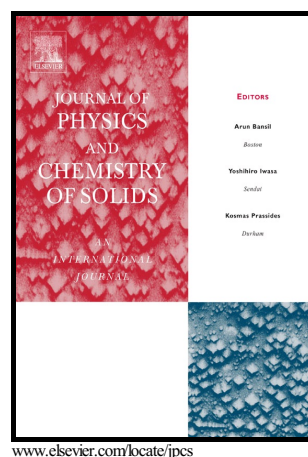


## Author's Accepted Manuscript

### Microwave-assisted Synthesis of Carbon-supported Carbides Catalysts for Hydrous Hydrazine Decomposition

Raman Mnatsakanyan, Alina R. Zhurnachyan, Valery A. Matyshak, Khachatur V. Manukyan, Alexander S. Mukasyan



PII: S0022-3697(16)30106-8  
DOI: <http://dx.doi.org/10.1016/j.jpcs.2016.05.008>  
Reference: PCS7780

To appear in: *Journal of Physical and Chemistry of Solids*

Received date: 25 January 2016  
Revised date: 12 May 2016  
Accepted date: 16 May 2016

Cite this article as: Raman Mnatsakanyan, Alina R. Zhurnachyan, Valery A. Matyshak, Khachatur V. Manukyan and Alexander S. Mukasyan, Microwave-assisted Synthesis of Carbon-supported Carbides Catalysts for Hydrous Hydrazine Decomposition, *Journal of Physical and Chemistry of Solids* <http://dx.doi.org/10.1016/j.jpcs.2016.05.008>

This is a PDF file of an unedited manuscript that has been accepted for publication. As a service to our customers we are providing this early version of the manuscript. The manuscript will undergo copyediting, typesetting, and a review of the resulting galley proof before it is published in its final citable form. Please note that during the production process errors may be discovered which could affect the content, and all legal disclaimers that apply to the journal pertain

# Microwave-assisted Synthesis of Carbon-supported Carbides Catalysts for Hydrous Hydrazine Decomposition

Raman Mnatsakanyan<sup>1\*</sup>, Alina R. Zhurnachyan<sup>1</sup>, Valery A. Matyshak<sup>2</sup>, Khachatur V.

Manukyan<sup>3\*</sup>, Alexander S. Mukasyan<sup>4</sup>

<sup>1</sup>Laboratory of Kinetics and Catalysis, Institute of Chemical Physics, National Academy of Sciences of the Republic of Armenia, Yerevan 0014, Armenia

<sup>2</sup>Laboratory of Heterogeneous Catalysis, N.N. Semenov Institute of Chemical Physics, Russian Academy of Sciences, 119991, Moscow, Russia

<sup>3</sup>Department of Physics, University of Notre Dame, Notre Dame, Indiana 46556, United States

<sup>4</sup>Department of Chemical and Biomolecular Engineering, University of Notre Dame, Notre Dame, Indiana 46556, United States

\*Corresponding author. Tel.: +574 631 6083. kmanukya@nd.edu

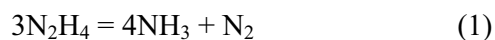
## Abstract

Microwave-assisted synthesis of carbon-supported Mo<sub>2</sub>C and WC nanomaterials was studied. Two different routes were utilized to prepare MoO<sub>3</sub> (WO<sub>3</sub>) - C precursors that were then subjected to microwave irradiation in an inert atmosphere. The effect of synthesis conditions, such as irradiation time and gas environment, was investigated. The structure and formation mechanism of the carbide phases were explored. As-synthesized nanomaterials exhibited catalytic activity for hydrous hydrazine (N<sub>2</sub>H<sub>4</sub>·H<sub>2</sub>O) decomposition at 30 – 70 °C. It was shown that the catalyst activity significantly increases if microwave irradiation is applied during the decomposition process. Such conditions permit complete conversion of hydrazine to ammonia and nitrogen within minutes. This effect can be attributed to the unique nanostructure of the catalysts that includes microwave absorbing carbon and active carbide constituents.

**Keywords:** carbides, microwave, synthesis, catalysts, hydrazine decomposition

## 1. Introduction

The catalytic decomposition of anhydrous hydrazine ( $N_2H_4$ ) has been of interest for many years since this process was successfully used as a monopropellant for satellite propulsion [1–6]. It was shown earlier [2,5–7] that the decomposition of hydrazine involves two routes:



The reaction pathway depends on the catalyst used and the temperature. Supported metal (Ni, Pd, and Pt) catalysts allow decomposition of anhydrous hydrazine even at room temperature [7]. With increasing temperature, the hydrogen selectivity (30–80 °C) increases first, and then quickly decreases. Above 400°C, the hydrogen selectivity tends to increase again due to the decomposition of ammonia. Transition metal carbides (e.g.  $Mo_2C$ , WC) catalysts are also active in the hydrazine decomposition reaction. For example, a WC catalyst prepared by a temperature-programmed reduction of  $WO_3$  with a  $CH_4/H_2$  mixture was thoroughly investigated [5]. The authors indicate that the excess of carbon on the WC surface inhibits  $N_2H_4$  decomposition while carbon removal improves the catalytic activity. Alumina-supported molybdenum carbide ( $Mo_2C$ ) catalysts were prepared by temperature-programmed reduction and tested in a monopropellant thruster [1]. This catalyst exhibited significant activity at 50-100 °C. A tungsten carbide - carbon nanotube catalyst was also fabricated by a microwave-assisted technique [4]. The as-prepared catalyst exhibits 100% hydrazine conversion at temperatures above 100 °C and demonstrates high hydrogen selectivity at 600 °C. Below 100 °C, the catalyst is selective for ammonia formation.

Catalytic decomposition of *hydrous hydrazine* ( $N_2H_4 \cdot H_2O$ ) is considered a promising process for hydrogen storage applications due to the large amount of available hydrogen (8.0 wt.%) in  $N_2H_4 \cdot H_2O$  [8–13]. Many metallic (Fe, Co, Ni, Cu, Ru, Rh, Ir, Pt and Pd)

nanoparticles exhibit measurable catalytic activity for the decomposition of hydrous hydrazine toward hydrogen at temperatures below 80 °C [10]. Among those catalysts, Rh nanoparticles were found to be the most selective (44%) for hydrogen release [14]. Bimetallic nanoparticles (e.g. Rh-Ni, Pt-Ni, Pd-Ni) show improved catalytic performance and higher hydrogen selectivity [15–20]. Noble-metal-free bimetallic Ni-Fe nanoparticles were remarkably active and selective towards hydrogen under moderate temperatures [21]. Highly dispersed Al<sub>2</sub>O<sub>3</sub>-supported Ni catalysts provided 100% conversion and high H<sub>2</sub> selectivity for the decomposition at room temperature [22,23]. The above analysis of the reported literature indicates that metallic catalysts permit *hydrous hydrazine* decomposition at relatively low temperatures. However, it is still unclear whether transition metal carbides (e.g. Mo<sub>2</sub>C, WC), are also able to catalyze the decomposition of *hydrous hydrazine* at such low temperatures.

Here, we report the microwave-assisted synthesis of carbon-supported nanostructured Mo<sub>2</sub>C and WC catalysts, which were tested for *hydrous hydrazine* decomposition at relatively low temperatures. We show that microwave irradiation significantly increases the activity of catalysts during hydrous hydrazine decomposition due to the unique combination of microwave absorbing carbon and active carbide nanoparticles. Such catalysts permit complete conversion of hydrous hydrazine to ammonia and nitrogen within minutes.

## 2. Materials & Methods

### 2.2. Preparation of catalysts

Two different routes were used to prepare MoO<sub>3</sub>-C and WO<sub>3</sub>-C catalyst precursors. Reactants in both routes were calculated assuming 70 wt.% of carbide loading in the catalysts. In the first route, 3 g of molybdenum (99.5% pure, the particle size of 10 μm) or tungsten (99.7% pure, the particle size of 2 μm) powders were dissolved in 100 ml of 15% hydrogen peroxide solution to obtain peroxy-complexes of corresponding metals. Then 1 ml isopropanol and 2 g

carbon (Vulcan XC-72) were added to the resulting solutions and slowly mixed using a magnetic stirrer for 30 min, and further homogenized ultrasonically for 10 min. The as-prepared slurries were dried at 80 °C. The resulting solids were heated to 250 °C for two hours in airflow to ensure decomposition of peroxy-complexes yielding carbon-supported MoO<sub>3</sub> or WO<sub>3</sub> precursors. In the second route, 5.5 g of ammonium molybdate tetrahydrate, (NH<sub>4</sub>)<sub>6</sub>Mo<sub>7</sub>O<sub>24</sub>·4H<sub>2</sub>O, was dissolved in 50 ml of deionized water. One ml of isopropanol and 2 g of carbon were added to the solution and mixed as in the previous route. Dried mixtures were then placed into a tube reactor and heated at 300 °C for four hours in nitrogen flow to prepare the MoO<sub>3</sub>-C precursor.

Microwave-assisted synthesis of carbon-supported metal carbides was performed in a quartz tube reactor in a nitrogen flow. The precursor was placed in the reactor, which was then purged with nitrogen for 0.5-2 h at room temperature. A microwave oven, with a frequency of 2.45 GHz and 900W, was used to irradiate the tube for up to 480 s. The set of microwave irradiation impulses with 20 s duration and with 5 s in between each impulse was used to avoid excessive heating of the samples.

## 2.2. Precursors and Catalysts Characterization

The crystallinity and phase composition of the catalysts were determined by X-ray diffraction (XRD) analysis with Ni-filtered Cu K $\alpha$  radiation (D8 Advance, Bruker or DRON3.0, Burivestnik) operated at 40 kV and 40 mA. BET specific surface area was determined by an ASAP 2020 apparatus (Micromeritics). Before analysis, the samples were dried at room temperature and then degassed in vacuum at 120 °C for 15 h.

Scanning (SEM) and transmission electron microscopy (TEM) were used to characterize the composition and morphology of the catalysts, as well as their atomic structure. The microstructural analysis was conducted in a field emission SEM Magellan 400 (FEI), with a resolution of 0.6 nm, which is also equipped with energy dispersive X-ray

spectrometer (EDS, Bruker) with an energy resolution of 123 eV. A Titan (FEI) transmission electron microscope (TEM) with a resolution of 0.136 nm in scanning TEM mode and about 0.1 nm information limit in high resolution TEM mode was also used. The Titan is equipped with an energy dispersive X-ray spectroscopy (EDS, Oxford Inc.) system with a spectral energy resolution of 130 eV.

A thermogravimetric analyzer and differential scanning calorimeter (DSC/TG, Setaram) coupled with a mass spectrometer (Pfeiffer Vacuum) were used to analyze the gasses that desorb during the heating of catalysts. In these experiments, 0.05 g of catalysts is heated to 600 °C at a 10 °C/min heating rate in an atmosphere of 99.99 % nitrogen with a flow rate of 20 cm<sup>3</sup>/min. The recording rate of evolved gases was 10 data points per second.

### *2.3. Catalytic experiments*

The catalytic tests were performed by placing 0.5 g of catalyst and 5 ml of diluted (1 M) solution of hydrous hydrazine into a preheated (70 °C) glass reactor for up to 8 min. After the experiment, the solid catalysts were rapidly separated from the solution, and the concentration of hydrous hydrazine was measured by iodometric titration according to the GOST protocol # 19503-88 [24]. Kinetics of hydrous hydrazine decomposition was investigated under microwave irradiation. In these experiments, 5 ml of 1 M hydrous hydrazine solution was poured into a Teflon-lined autoclave with a volume of 65 cm<sup>3</sup> and then 0.5 g of catalyst powder was added. The closed autoclave was placed in the microwave oven. Continuous microwave irradiation of autoclave at the power of 180 W was performed for 10-240 s. The autoclave was opened, and the temperature of the solution was measured by inserting a K-type thermocouple probe. Such measurements revealed that 3 min of microwave irradiation increases the temperature of the solution to ~70 °C.

### 3. Results and discussion

#### 3.1. Synthesis and characterization of catalysts

The effects of gas environment, duration of irradiation, as well as composition of the precursors, are optimized for the preparation of catalysts. At minimum, two hours of nitrogen flow for is necessary to obtain desired metal carbide – carbon catalysts. Shorter purge durations result in products that consist of metal oxides and carbides. The presence of oxygen during synthesis leads to oxidation of carbon and reduces the quantity of carbide phases.

The influence of microwave irradiation duration on the composition of the product was first studied using initial mixtures prepared from ammonium molybdate (AM). Figure 1A shows that after 0.5 min of irradiation the sample consists of  $\text{MoO}_3$ ,  $\text{MoO}_2$  and  $\text{Mo}_2\text{C}$  phases. After 1 min of irradiation, the diffraction peaks of  $\text{MoO}_3$  disappeared, and the intensity of  $\text{MoO}_2$  peaks decreased significantly. The sample treated for 2 min primarily consists of the  $\text{Mo}_2\text{C}$  and trace  $\text{MoO}_2$  (Figure 1A). The experiments using a peroxo-complex (PC) of Mo as precursor exhibited similar results (not shown) with partial reduction of  $\text{MoO}_3$  to  $\text{MoO}_2$  and subsequent formation of  $\text{Mo}_2\text{C}$ . XRD pattern of a product with peroxo-complex precursor irradiated for 3 min shows only  $\text{Mo}_2\text{C}$  peaks (Figure 1A).

The phase formation sequence in WC-forming system is different as compared to  $\text{Mo}_2\text{C}$ . Figure 1B demonstrates that 3 min irradiation of tungsten peroxo-complex precursor results in a product that consists of W,  $\text{W}_2\text{C}$  and WC. Pure-phase WC can be produced only after 8 minutes of irradiation.

*In situ* thermogravimetry and mass spectrometry were used to study thermal desorption characteristics of catalysts. The results of these analyses show that  $\text{Mo}_2\text{C}$ -C catalyst (prepared by ammonium molybdate) contains significant amounts of adsorbed carbon dioxide (Figure 2A). Mass-spectroscopy provides evidence that desorption peaks of  $\text{CO}_2$  (m/z numbers of 44, 28 and 16) are located at ~250, 370, and 570 °C. Stepwise desorption of  $\text{CO}_2$

indicates that the surface of the catalyst is energetically non-uniform. This result also evidenced that the chemisorbed  $\text{CO}_2$  on the surface of catalysts exists at least in three different forms. Thermogravimetric analysis shows that, upon heating, the carbide catalysts lose much more weight than the initial carbon (Figure 2B).

SEM images of initial carbon nanoparticles and catalysts are summarized in Figure 3. The size of initial carbon nanoparticles is  $\sim 50$  nm (Figure 3A). The catalyst produced from the ammonium molybdate precursor after 2 min of irradiation has similar sizes of carbon nanoparticles (Figure 3B). Figure 3C indicates that the sample fabricated from the molybdenum peroxo-complex precursor (with 3 min irradiation time) has slightly larger particles (50-70 nm). The particle size of optimized WC-C catalysts (8 min of irradiation time) is in the range of 300-500 nm (Figure 3D).

The results of TEM analysis of  $\text{Mo}_2\text{C}$ -C catalyst prepared from a molybdenum peroxo-complex precursor is shown in Figure 4. Selected area diffraction (SAD) pattern (inset in Figure 4A) and EDS analysis suggests that the lighter particles (SAD, in upper left corner) are amorphous carbon, while darker nanoparticles (SAD, left lower corner) are the crystalline  $\text{Mo}_2\text{C}$  phase. High-magnification TEM images demonstrate that the sizes of  $\text{Mo}_2\text{C}$  and carbon nanoparticles are indeed comparable (Figure 4B). Both Figure 4A and 4B indicate that  $\text{Mo}_2\text{C}$  and carbon nanoparticles are anchored to each other. However, high-resolution TEM images of carbon (Figure 4C) and  $\text{Mo}_2\text{C}$  (Figure 4D) nanoparticles exhibit significant differences in structure. Carbon nanoparticles are amorphous and highly porous with pore sizes 0.5-0.7 nm, while  $\text{Mo}_2\text{C}$  nanoparticles are crystalline and free of pores.

BET surface area data of initial carbon is  $204 \text{ m}^2/\text{g}$  (Table 1). The surface area of  $\text{Mo}_2\text{C}$ -C catalysts is 32 and  $24 \text{ m}^2/\text{g}$  for ammonium molybdate and peroxo-complex precursors, respectively. The lowest surface area,  $10 \text{ m}^2/\text{g}$ , is exhibited by the WC-C catalyst prepared from peroxo-complex precursor for 8 min of microwave irradiation. The differences

in the surface area of the carbon and products are more pronounced as compared to their particle sizes. It should be noted that the surface area of pure carbon after 3 min of microwave irradiation decreases from 204 to 149 m<sup>2</sup>/g. This result indicates that microwave heating alone is not the major factor contributing to the severe decrease in surface area of products.

Nitrogen adsorption/desorption curves for carbon, irradiated carbon and Mo<sub>2</sub>C-C catalysts (Figure 5) have the characteristic feature of Type III isotherm according to IUPAC classification with a narrow hysteresis loop. Isotherms of such shape indicate the presence of micropores while a small hysteresis loop suggest evidence of some mesopores too. Nearly identical shapes of isotherms suggest that nitrogen adsorption in Mo<sub>2</sub>C-C catalysts predominantly takes place in porous carbon nanoparticles. As the total volume of carbon nanoparticles decreases due to the formation of pore-free Mo<sub>2</sub>C nanoparticles, the sample adsorbs less nitrogen.

It is known that the vapor pressure of MoO<sub>3</sub> at temperatures in the range 400 - 600°C is relatively high (0.1 – 0.5 kPa) [25]. Earlier works [26],[27] suggest that carbon reduces MoO<sub>3</sub> at this temperatures by the following reaction:



Our TEM studies reveal that Mo<sub>2</sub>C nanoparticles are pore-free and have similar sizes to the initial carbon nanoparticles. This finding and a significant decrease in the surface area of the product allowed us to hypothesize that MoO<sub>3</sub> vapor infiltrates into the porous carbon nanoparticles, and MoO<sub>2</sub> grows inside the pores via reaction 3 (see Figure 6). It was also shown previously that MoO<sub>2</sub> further reduces to molybdenum followed by formation of Mo<sub>2</sub>C at 650-900 °C [27]. In our study, the intermediate Mo phase has not been observed during microwave-assisted synthesis (Figure 1). It is possible that, following solid-state carbidization,

the reaction may be significantly accelerated due to the shorter diffusion distances of MoO<sub>2</sub> and carbon inside MoO<sub>2</sub>/C composite particles (Figure 6):



In contrast to Mo<sub>2</sub>C, the formation of WC occurs by a different pathway. XRD analysis shows the multistage conversion of WO<sub>3</sub> to WC through W and W<sub>2</sub>C phases that is consistent with previously reported data [28-30]. It should be noted that vapor pressure of WO<sub>3</sub> at 700-1000 °C is only ~10<sup>-4</sup> kPa<sup>24</sup>. Therefore, the reduction of WO<sub>3</sub> to W is slow. It was also shown that the synthesis of WC using the WO<sub>3</sub>+C mixture can be achieved only at 900-1000 °C [28]. Clearly, longer microwave irradiation significantly decreases the porosity of the carbon nanoparticles and creates an additional diffusion limitation during the carbide formation stage.

### 3.2. Catalytic activity

The catalytic activities of Mo<sub>2</sub>C-C and WC-C for hydrous hydrazine decomposition were investigated in the temperature range 25-70 °C. Both catalysts show conversion of hydrazine at temperatures above 50 °C. Kinetics of hydrazine decomposition for catalysts at 70°C are shown in Figure 7. These data indicate that for Mo<sub>2</sub>C-C catalysts, conversion of hydrazine increases linearly to ~20% during the first 4 min of the process. In the case of WC-C catalyst, the maximum conversion (10%) is reached in 4 min. It should be noted that the loading of the carbide phase in both catalysts is ~70 wt% indicating that Mo<sub>2</sub>C has higher catalytic activity as compared to WC. Such a distinct difference of catalytic activities may be attributed to the significantly smaller particle size of Mo<sub>2</sub>C relative to WC (Figure 2). Gas chromatography analysis of effluents reveals the presence of ammonia and nitrogen indicating incomplete decomposition of hydrous hydrazine by reaction (1). Irradiated carbon nanoparticles are not

active for hydrazine decomposition at the studied temperatures. This means that the activity of the investigated catalysts is related to the carbide phases only.

We have studied the microwave-assisted catalytic decomposition of hydrous hydrazine (Figure 7). These results demonstrate that microwave irradiation with 180W power leads to a significant increase in the activity of both catalysts. It can be seen that hydrazine fully decomposes within 4 min of irradiation using Mo<sub>2</sub>C-C catalysts while conversion for WC-C catalysis is ~55%. It is worth noting that the results of the effluent gas analysis show ammonia and nitrogen again, as main gas products. Also, microwave-assisted catalytic experiments indicate that pure carbon is active for hydrazine decomposition. However, conversion of hydrazine is less than 5% during 4 min of the process.

We postulated that the significant increase in catalytic activity in microwave-assisted experiments was related to the combination of the carbon nanostructure and active carbide phase. Previously, similar carbon - ceramic nanoparticles composites with unusual catalytic and gas-sensing properties were also reported [31,32]. Indeed, carbon is known as an excellent absorber of microwave irradiation [33]. Therefore, the local temperature on the surface of catalysts during microwave irradiation may be higher than the average temperature of the hydrazine solution.

#### 4. Conclusions

Microwave irradiation permits controllable synthesis of Mo<sub>2</sub>C-C and WC-C nanomaterials. Microwave heating allows rapid vaporization of MoO<sub>3</sub> precursors that react with microporous carbon resulting in MoO<sub>2</sub>/C composite powders, followed by formation of the Mo<sub>2</sub>C phase. In the WO<sub>3</sub>-C system, the conversion of WO<sub>3</sub> to WC requires longer irradiation due to the formation of W and W<sub>2</sub>C intermediate phases. Mo<sub>2</sub>C-C and WC-C nanomaterials exhibited catalytic activity for hydrous hydrazine (N<sub>2</sub>H<sub>4</sub>·H<sub>2</sub>O) decomposition at 30-70 °C.

The activity of catalysts increases significantly if microwave irradiation is applied during the decomposition process. This effect is related to the selective heating of catalysts which contain microwave absorbing carbon and active carbide nanoparticles.

### Acknowledgments

Support from NFSAT and CRDF Global (Project # YSSP 13-21) is acknowledged. The Author also would like to thank Sergei Rouvimov (Notre Dame Imaging integrated facility, at University of Notre Dame) for his assistance in TEM analysis.

### References

- [1] X. Chen, T. Zhang, P. Ying, M. Zheng, W. Wu, L. Xia, T. Li, X. Wang and C. Li, *Chem. Commun.* (2002) 288–289.
- [2] X. Chen, T. Zhang, M. Zheng, Z. Wu, W. Wu, C. Li, *J. Catal.* 224 (2004) 473–478.
- [3] X. Chen, T. Zhang, M. Zheng, L. Xia, T. Li, W. Wu, X. Wang and C. Li, *Ind. Eng. Chem. Res.* 43 (2004) 6040–6047.
- [4] C. Liang, L. Ding, A. Wang, M. Zhiqiang, J. Qiu, T. Zhang, *Ind. Eng. Chem. Res.* 48 (2009) 3244–3248.
- [5] J.B.O. Santos, G.P. Valeca, R. J.A.J. Rodrigues, *J. Catal.* 210 (2002) 1–6.
- [6] M. Zheng, X. Chen, R. Cheng, N. Li, J. Sun, X. Wang, T. Zhang, *Catal. Commun.* 7 (2006) 187–191.
- [7] M. Zheng, R. Cheng, X. Chen, N. Li, L. Li, X. Wang, T. Zhang, *Int. J. Hydrogen Energy.* 30 (2005) 1081–1089.
- [8] S.K. Singh, Q. Xu, *J. Am. Chem. Soc.* 131 (2009) 18032–18033.
- [9] H.L. Jiang, S.K. Singh, J.M. Yan, X.B. Zhang, Q. Xu, *ChemSusChem.* 3 (2010) 541–549.

- [10] M. Yadav, Q. Xu, , *Energy Environ. Sci.* (2012) 9698–9725.
- [11] R. Lan, J.T.S. Irvine, S. Tao, *Int. J. Hydrogen Energy.* 37 (2012) 1482–1494.
- [12] S.K. Singh, Q. Xu, *Catal. Sci. Technol.* 3 (2013) 1889–1900.
- [13] K. V. Manukyan, A. Cross, S. Rouvimov, J. Miller, A.S. Mukasyan, E.E. Wolf, *Appl. Catal. A Gen.* 476 (2014) 47–53.
- [14] S.K. Singh, Y. Iizuka, Q. Xu, *Int. J. Hydrogen Energy.* 36 (2011) 11794–11801.
- [15] S.K. Singh, Q. Xu, *Chem. Commun.* 46 (2010) 6545–6547.
- [16] S.K. Singh, Q. Xu, *Inorg. Chem.* 49 (2010) 6148–6152.
- [17] J. Wang, X.-B. Zhang, Z.-L. Wang, L.-M. Wang, Y. Zhang, *Energy Environ. Sci.* 5 (2012) 6885–6888
- [18] A.K. Singh, Q. Xu, *Int. J. Hydrogen Energy.* 39 (2014) 9128–9134.
- [19] Y. Du, J. Su, W. Luo, G. Cheng, *ACS Appl. Mater. Interfaces.* 7 (2015) 1031–1034.
- [20] Y. Jiang, Q. Kang, J. Zhang, H.-B. Dai, P. Wang, *J. Power Sources.* 273 (2015) 554–560.
- [21] S.K. Singh, A.K. Singh, K. Aranishi, Q. Xu, *J. Am. Chem. Soc.* 133 (2011) 19638–19641.
- [22] L. He, Y. Huang, A. Wang, X. Wang, X. Chen, J.J. Delgado, T. Zhang, *Angew. Chemie - Int. Ed.* 51 (2012) 6191–6194.
- [23] L. He, Y. Huang, A. Wang, Y. Liu, X. Liu, X. Chen, J.J. Delgado, X. Wang, Tao Zhang, *J. Catal.* 298 (2013) 1–9.
- [24] Hydrazine-hydrate for industrial use. Specifications (GOST #19503-88), L14 (1993) 1–17.
- [25] E.K. Kazenas, D.M. Chijikov, Pressure and composition of the vapor above the oxides of chemical elements (in Russian), Nauka, Moscow, 1976.
- [26] S.V. Aydinyan, Z. Gumruyan, K.V. Manukyan, S.L. Kharatyan, *Mater. Sci. Eng. B.*

- 172 (2010) 267–271.
- [27] K.V. Manukyan, S. Aydinyan, A. Aghajanyan, Y. Grigoryan, O. Niazyan, S. Kharatyan, *Int. J. Refract. Met. Hard Mater.* 31 (2012) 28–32.
- [28] G.A. Swift, Koc Rasit, *J. Mater. S.* 36 (2001) 803 – 806.
- [29] K.G. Kirakosyan, K.V. Manukyan, S.L. Kharatyan, R. A. Mnatsakanyan, *Mater. Chem. Phys.* 110 (2008) 454–456.
- [30] A.R. Zurnachyan, K.V. Manukyan, S.L. Kharatyan, V.A. Matyshak, R.A. Mnatsakanyan, *Kinet. Catal.* 52 (2011) 851–854.
- [31] X. Wang, H. Fan, P. Ren, M. Li, *Mater. Res. Bull.* 50 (2014) 191–196.
- [32] H. Tian, H. Fan, H. Guo, N. Song, *Sensors Actuators, B Chem.* 195 (2014) 132–139.
- [33] S. Horikoshi, N. Serpone, *Catal. Sci. Technol.* 4 (2014) 1197-1210.

### Figure Captions

Figure 1 Results of XRD analysis of Mo<sub>2</sub>C-C (A) and WC-C (B) catalysts synthesized at different microwave irradiation duration utilizing ammonium molybdate (AM) and peroxy-complex (PC) precursors.

Figure 2 Dynamic mass-spectrometry (A) of gases release during heating of Mo<sub>2</sub>C-C catalyst (mass-to-charge ratios of 16, 28, and 44 indicate CO<sub>2</sub> realize) and thermo-gravimetric analysis (B) of the catalysts.

Figure 3 SEM images of carbon (A), Mo<sub>2</sub>C synthesized utilizing ammonium molybdate with 2 min irradiation (B) and Mo peroxy-complex (C) precursor with 2 min of irradiation, and WC synthesized using tungsten peroxy-complex with 8 min of irradiation (D).

Figure 4 Results of TEM analysis of Mo<sub>2</sub>C-C catalyst: Bright field image with selected area diffraction patterns (A), high magnification TEM image of Mo<sub>2</sub>C and carbon nanoparticles as well as their high resolution TEM images, respectively.

Figure 5 Nitrogen adsorption (solid symbols) and desorption isotherms (open symbols) for initial carbon (curve *a*), carbon after 2 min of microwave irradiation (*b*) and Mo<sub>2</sub>C-C catalyst (*c*) synthesized using ammonium molybdate recourse.

Figure 6 Schematic representation of phase formation mechanism during microwave-assisted synthesis of Mo<sub>2</sub>C.

Figure 7 Conversion of hydrous hydrazine.

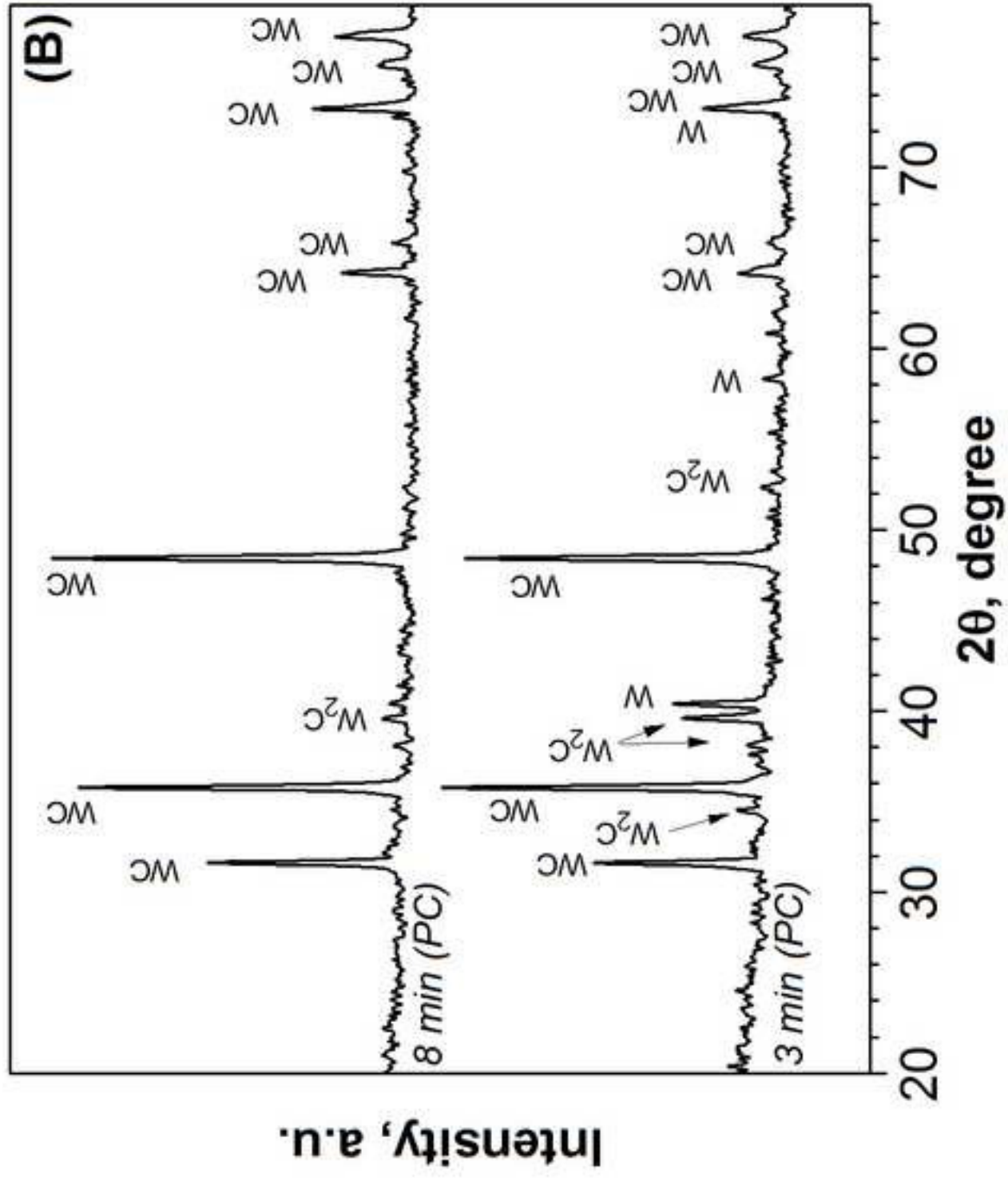
Table 1 Surface area of initial carbon and catalysts

<b>Material</b>	<b>Precursor</b>	<b>Duration of microwave irradiation, min</b>	<b>Surface area, m<sup>2</sup>/g</b>
<b>Carbon</b>	Initial	0	204
<b>Carbon</b>	Initial	3	149
<b>Mo<sub>2</sub>C-C</b>	Ammonium molybdate	2	32
<b>Mo<sub>2</sub>C-C</b>	Peroxy-complex of molybdenum	3	24
<b>WC-C</b>	Peroxy-complex of tungsten	8	10

### Highlights

- Microwave-assisted synthesis of Mo<sub>2</sub>C-C and WC-C nanomaterials is reported.
- Two different mechanisms of syntheses of carbide phase are proposed.
- Carbon-supported carbides are highly active in hydrazine decomposition reaction.





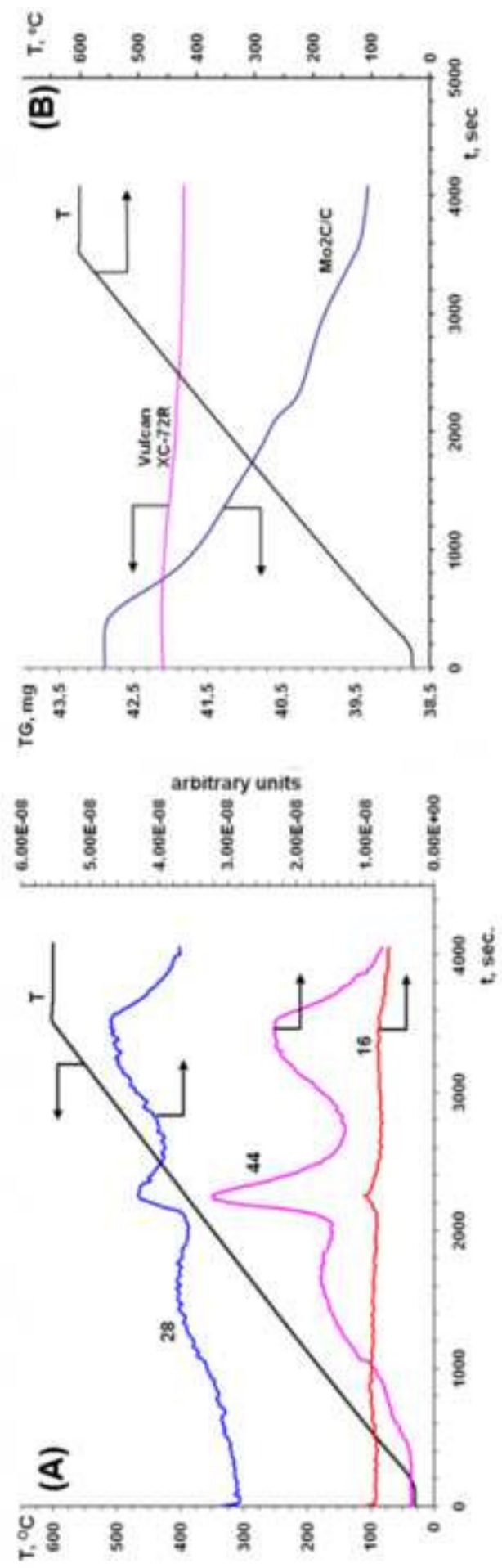


Figure 2

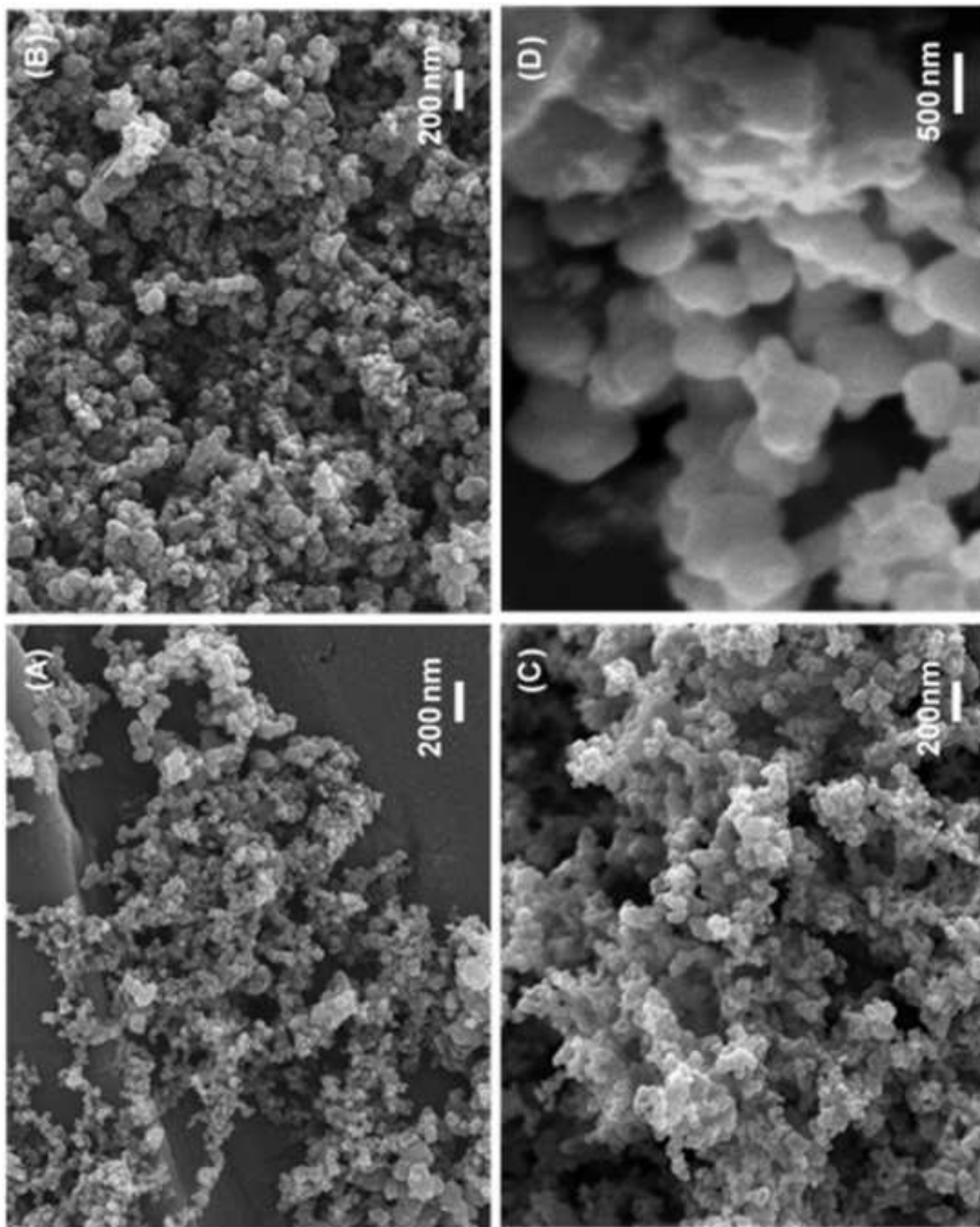


Figure 3

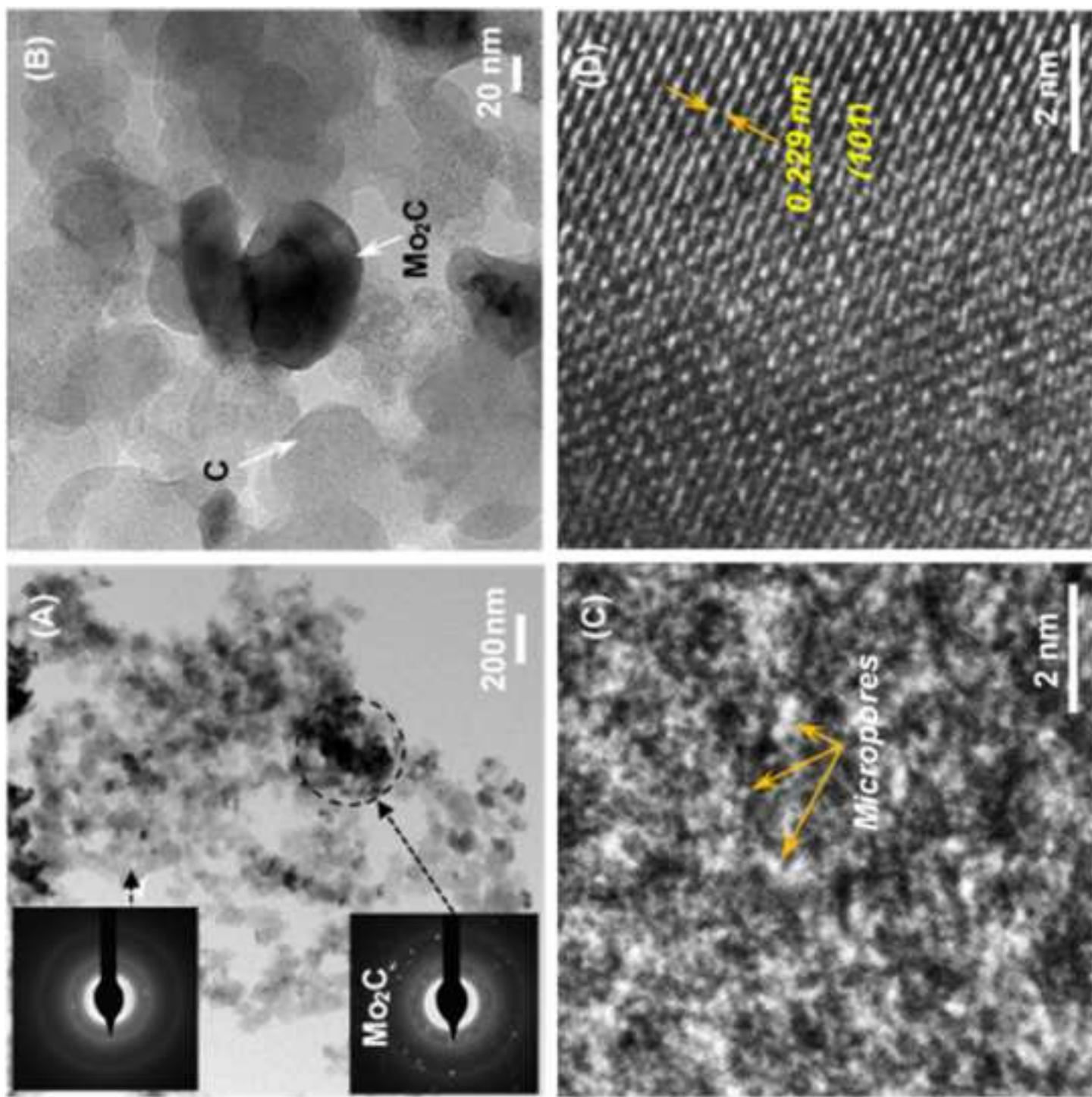


Figure 4

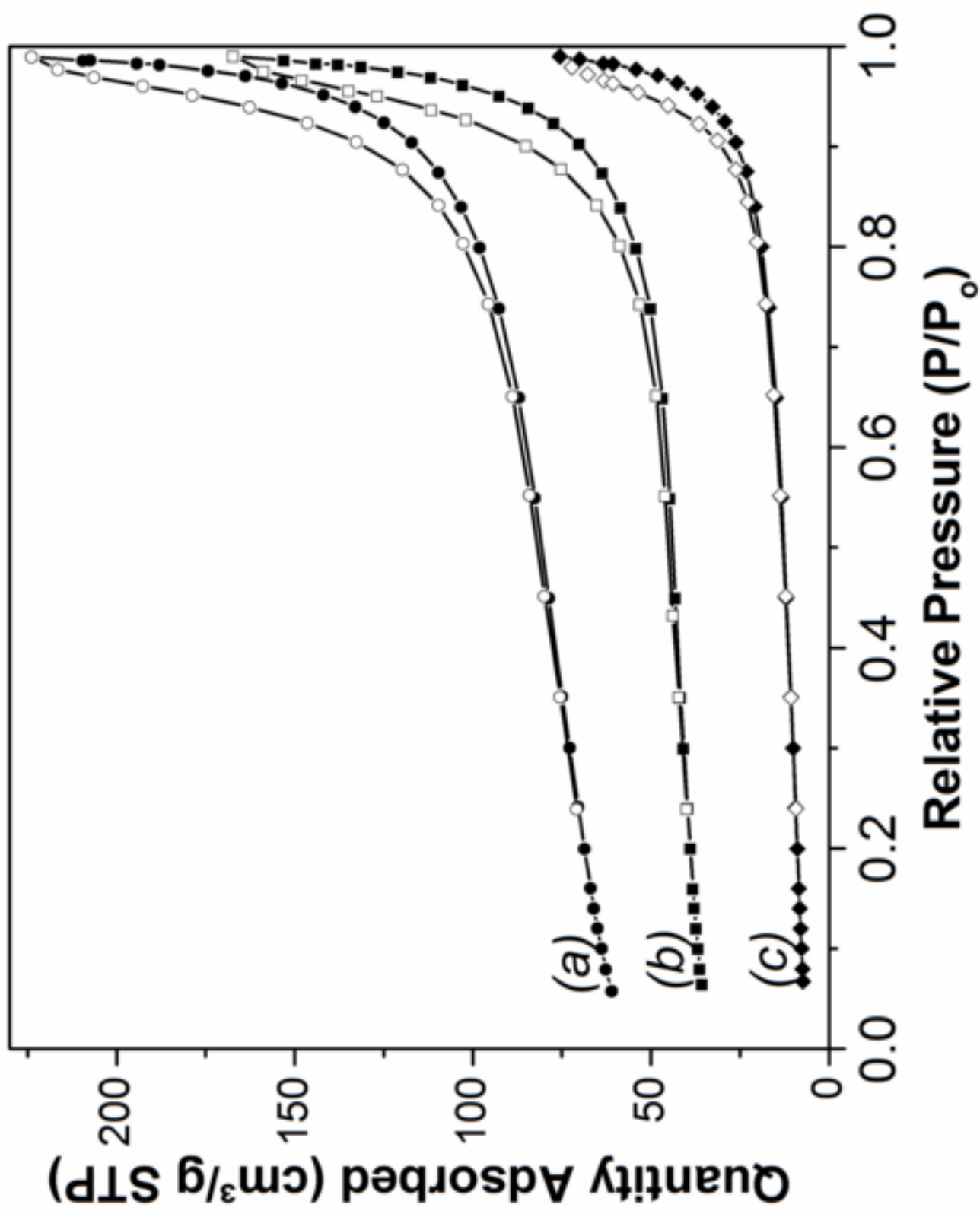
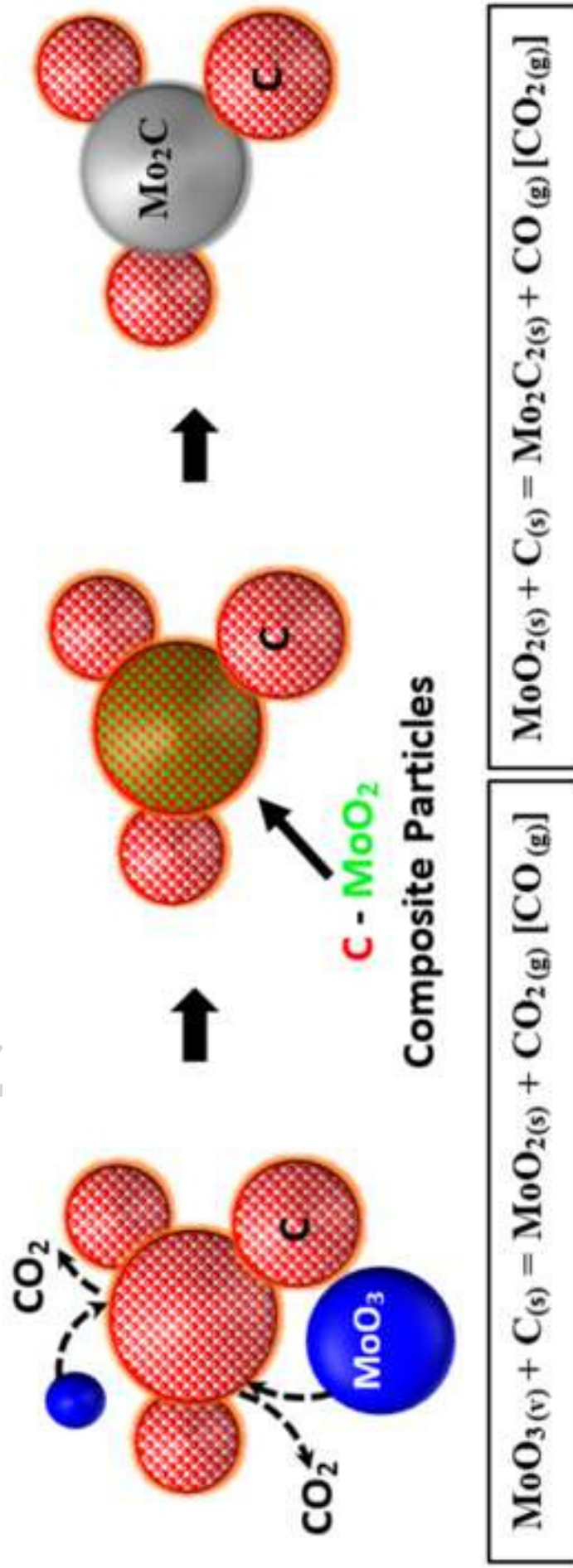


Figure 5



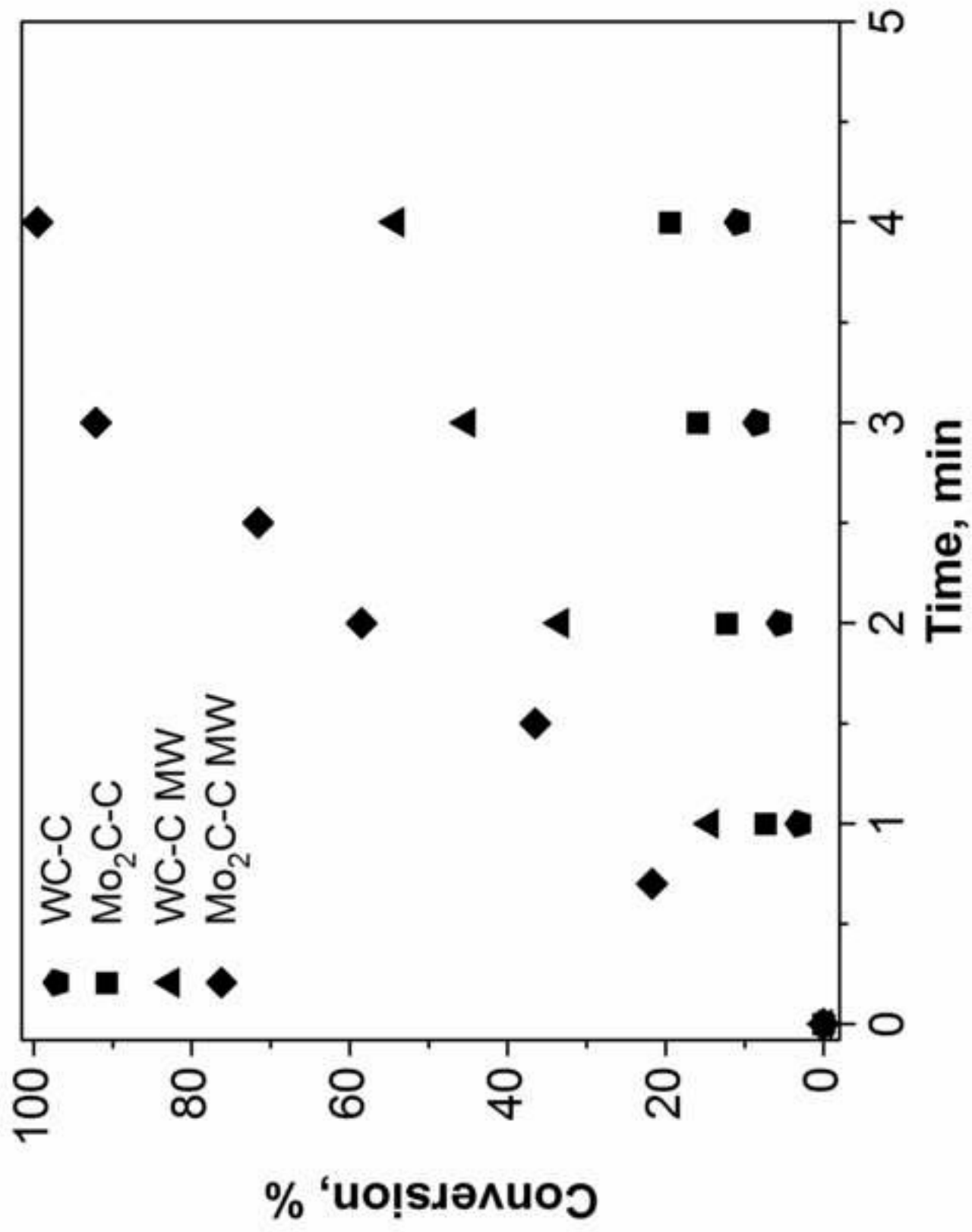


Figure 7